PGSE-NMR and SANS studies of the interaction of model polymer therapeutics with mucin

ARTICLE *in* BIOMACROMOLECULES · DECEMBER 2009

Impact Factor: 5.75 · DOI: 10.1021/bm9009667 · Source: PubMed

PGSE-NMR and SANS Studies of the Interaction of Model Polymer Therapeutics with Mucin

Peter Charles Griffiths,*,† Paola Occhipinti,†,‡ Christopher Morris,‡ Richard K. Heenan,§ Stephen Michael King,§ and Mark Gumbleton‡

School of Chemistry, Cardiff University, Main Building, Park Place, Cardiff CF10 3AT, United Kingdom, Welsh School of Pharmacy, Cardiff University, Redwood Building, King Edward VII Avenue, Cardiff CF10 3NB, United Kingdom, and ISIS Facility, Science and Technology Facilities Council, Rutherford Appleton Laboratory, Didcot OX11 0QX, United Kingdom

Received August 25, 2009; Revised Manuscript Received November 6, 2009

The viscous mucus coating that adheres to the epithelial surfaces of mammalian organs provides protection for the underlying tissues and is an efficient barrier to drug delivery. Pulsed-gradient spin−echo NMR and small-angle neutron scattering have been used to study the aqueous solution interaction of various model polymer therapeutics with mucin, the principle organic component within mucus. Nonionic polymers such as linear and star-branched poly(ethylene oxide) (PEO) and dextrin showed no appreciable interaction with mucin but suffered a moderate retardation in their rate of diffusion through the mucin solution. A strong interaction with mucin was observed for a series of polyamidoamine (PAMAM) dendrimers and hyperbranched poly(ethylene imine) (PEI), which displayed a characteristic pH-dependent profile and led to significant reductions in their rates of diffusion. These observations have implications for the design of optimized polymer therapeutic structures being adopted for the delivery of therapeutic moieties through mucin-rich environments.

Introduction

Significant progress has indeed been made over the past decade in the design and development of polymer-based nanosized hybrid therapeutics with several such delivery systems entering clinical trials but many challenges remain.[1]

Epithelial surfaces in mammalian organs (e.g., conductive airways of the lung and the gastrointestinal and reproductive tract) bear a mucus coating, a complex mixture of glycoprotein, lipid, and electrolytes that provides protection for the underlying cells and, therefore, represents an inherently efficient barrier to drug delivery. The efficacy of this barrier depends on its physicochemical state such as hydration and mucin content, which in turn is defined by its site of secretion and the presence of any disease (e.g., cystic fibrosis), all of which are factors that can affect the absorptive pharmacokinetics of the therapeutic agent.[2]

Mucus is in essence a water-rich biogel, the main components being water (up to 95%), mucin (generally no more than 5%), inorganic salts (about 1%), carbohydrates, and lipids. Mucin consists of high-molecular-weight (ranging from 500 to 20 000 kg mol^{-1}) O-linked glycoproteins (of varying length scales from a few hundred nanometers up to several micrometers) in turn composed of glycosylated and nonglycosylated peptide blocks linked by intramolecular disulfide bridges,[3] calcium ion or peptide cross-linking,[4] carbohydrate−carbohydrate bonds, and hydrophobic associations.[5] Mucins have a low isoelectric point (IEP $\approx$ 2 to 3) because of the anionic nature of their oligosaccharide side chains (sulfate and sialic acid units).

Several models have been invoked to describe the solution structure of mucin; aggregates of rod-shaped molecules comprising a central linear polypeptide core of 100 000 < M_w < 250 000 g mol^{-1} with radial oligosaccharide side chains of 2 to 12 monosaccharide residues attached to serine and threonine residues by O-glycosidic linkages,[6] a solvated random coil of flexible linear glycoprotein[7] that is either stiffened by the glycosylated fragments[8] or their interaction (the so-called "zipper" or bottle-brush model),[9] liquid crystalline structures,[7] and a double globule comb structure.[10] This complexity is compounded by the tendency of mucin to aggregate at low concentrations (and pH).

The aim of this study is to examine by pulsed-gradient spin−echo NMR (PGSE-NMR), the diffusion of a series of water-soluble polymers intended to represent model polymer therapeutics within mucin solutions and to quantify by small-angle neutron scattering (SANS) changes induced in the structure of mucin by the addition of that second polymer.

Material and Methods

Materials. Dried porcine gastric mucin (PGM) type III was purchased from Sigma Aldrich and used without any further treatment. Over the concentration range 0.5 < [mucin] < 5 wt %, solutions of PGM are viscous (Figure S1 in the Supporting Information) and exhibit a pronounced concentration dependence ($\eta \propto [\text{mucin}]^2$) but do not form gels. There is no pronounced sol−gel transition (Figure S2 in the Supporting Information), as has been reported previously for commercial samples of mucin. A series of water-soluble polymers, termed the "probe" polymer, have been examined in the presence of PGM, and these also were not further purified: linear PEO (l-PEG10K) nominal molecular weight M_w = 10 000 g mol^{-1} (Sigma-Aldrich, U.K.); linear deuterated PEO nominal molecular weight M_w = 10 000 g mol^{-1} (Polymer Laboratories, U.K.); linear PEO (l-PEG100K) nominal molecular weight M_w = 100 000 g mol^{-1} (Sigma-Aldrich, U.K.); branched polyethylenimine (b-PEI2K) nominal molecular weight M_w = 2000 g mol^{-1} (Sigma-Aldrich, U.K.); branched polyethylenimine (b-PEI25K) nominal molecular weight M_w = 25 000 g mol^{-1} (Sigma

* To whom correspondence should be addressed. Tel: +44-29 20875858. Fax: +44-29 20874030. E-mail: griffithspc@cardiff.ac.uk.
† School of Chemistry, Cardiff University.
‡ Welsh School of Pharmacy, Cardiff University.
§ Rutherford Appleton Laboratory.

10.1021/bm9009667
Published on Web 12/01/2009

Aldrich, U.K.); polyamidoamine dendrimer G2.0 (PAMAM G2.0) nominal molecular weight $M_w = 3260$ g mol^{-1} (Dendritech); polyamidoamine dendrimer G4.0 (PAMAM G4.0) nominal molecular weight $M_w = 14\,210$ g mol^{-1} (Dendritech); polyamidoamine dendrimer G3.5 (PAMAM G3.5) nominal molecular weight $M_w = 12\,930$ g mol^{-1} (Dendritech); polyamidoamine dendrimer G5.5 (PAMAM G5.5) nominal molecular weight $M_w = 52\,900$ g mol^{-1} (Dendritech); dextrin (type 1, corn) nominal molecular weight $M_w = 60\,000$ g/mol (ML laboratories, Keele, U.K.).

Preparation of Polymer−Mucin Solutions. Solutions were prepared with different mucin concentrations (1 wt % < [mucin] < 5 wt %) and a constant probe polymer concentration (0.5 wt %) by simply dissolving the required masses of polymer in D_2O (99.5 atom % D). Samples were left for at least 2 h but typically overnight at room temperature to allow full dissolution and equilibration. The solutions were not filtered, and the pH was adjusted by the addition of HCl or NaOH.

Small-Angle Neutron Scattering. SANS experiments were performed on the fixed-geometry, time-of flight LOQ diffractometer at the ISIS Spallation Neutron Source, Rutherford Appleton Laboratory, Didcot, U.K. A $Q = (4\pi/\lambda)\sin(\theta/2)$ range between 0.008 and 0.25 Å^{-1} is obtained by using neutron wavelengths (λ) spanning 2.2 to 10 Å with a fixed sample−detector distance of 4.1 m. The samples were contained in 2 mm path length, UV-spectrophotometer grade, quartz cuvettes (Hellma, GmBh) and mounted in aluminum holders on top of an enclosed, computer-controlled, sample chamber. Sample volumes were ~0.6 cm^3. All experiments were conducted at 37 °C (unless otherwise stated). Temperature control was achieved by using a thermostatted circulating bath pumping fluid through the base of the sample chamber, achieving a temperature stability of ±0.2 °C. Experimental measuring times were approximately 30−40 min.

All scattering data were (a) normalized for the sample transmission, (b) background corrected using a quartz cell filled with D_2O, and (c) corrected for the linearity and efficiency of the detector response using the instrument specific software package.

Pulsed-Gradient Spin−Echo NMR (PGSE-NMR). Pulsed-gradient spin−echo NMR experiments were carried out on a Bruker AMX360 NMR spectrometer operating at 360 MHz (^{1}H) and using a stimulated echo sequence, as described elsewhere.[11] For each measurement, a 5 mm diffusion probe and a Bruker gradient spectroscopy accessory unit was used. All experiments were conducted at 37 °C. Temperature stability was maintained by the standard air heating/cooling system of the spectrometer to an accuracy of ±0.3 °C.

Two approaches to analyzing the data were employed; where there is little spectral overlap with the peaks of interest (e.g., PAMAMs in mucin), the diffusion coefficients have been extracted by an analysis of the peak integrals; however, where spectral overlap is pronounced (e.g., PEG in mucin), a more involved component-resolved (CORE) approach (Figure S3 in the Supporting Information) was adopted.[12]

In both cases, the self-diffusion coefficient D_s was extracted from an analysis of the peak amplitudes according to eq 1

$$A(\delta, G, \Delta) = A_o \exp[(-kD_s)] \quad (1)$$

where A is the peak amplitude in the absence (A_o) or the presence of trapezoidal field gradient pulses of duration δ (400 μs < δ < 2.8 ms), ramp time σ (250 μs) strength G (0.86 T m^{-1}) and separation Δ (140 ms), and k is given by eq 2

$$k = -\gamma^2 G^2 \left(\frac{30\Delta(\delta + \sigma)^2 - (10\delta^3 + 30\sigma\delta^2 + 35\sigma^2\delta + 14\delta^3)}{30} \right) \quad (2)$$

where γ is the gyromagnetic ratio.

Results

In this current work, PGSE-NMR has been used to quantify the diffusion of model polymer therapeutics (the "probe" polymer) within aqueous mucin solutions. SANS has been used to detect any perturbation in the mucin solution structure induced by the addition of the probe polymer and thus to provide a complementary indication of any interaction between the mucin and probe polymer. However, we first present the SANS analysis of simple mucin solutions, subsequently, that from mixtures of mucin−probe polymer, before elaborating on the PGSE-NMR study.

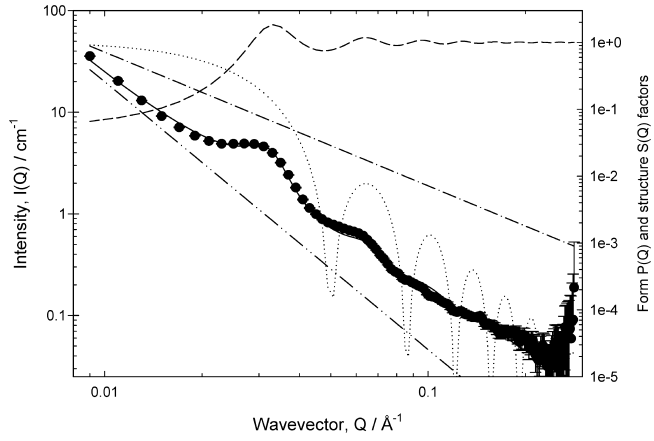

Figure 1. Scattering from mucin 5 wt % (closed circles) at 37 °C, pH 7; fitting to the scattering data (solid line); globule form factor $P(Q)$ (dotted line); globule structure factor $S(Q)$ (dashed line); Q^{-2} (dashed-dotted line); and Q^{-4} (dashed-dotted-dotted line) terms. The final data points have been omitted for clarity.

SANS from PGM Solutions. The SANS from 5 wt % (50 mg mL^{-1}) (nonpurified) porcine gastric mucin PGM solutions at 37 °C is presented in Figure 1. As may be seen, there are a number of features in the data, including pronounced maxima against a slowly decaying background signal. The maxima arise as a result of the interference from scattering centers within the solution, implying some level of order. The spacing (ξ) associated with these maxima scale with concentration ($\xi \propto c^{-0.38\,(\pm 0.03)}$ (over the entire range studied 1 < [mucin] < 5 wt %)) characteristic of liquid-like ordering ($\xi \propto c^{-1/3}$) (Figure S4 in the Supporting Information). These maxima are still present in the scattering, even at concentrations as low as 1 wt % (10 mg mL^{-1}). These features are more pronounced than those in the SANS (and SAXS) studies of Waigh et al.[10,13−16] Interestingly, the peak does not move with increasing ionic strength (ambient < [salt] < 0.1 M NaCl, where on the basis of conductivity measurements the ambient ionic strength is comparable to ~10 mM NaCl), implying that they do not arise as a result of an electrostatic structure factor (Figure S5 in the Supporting Information).

In their early SANS study, Waigh et al.[16] interpreted their data in terms of representing mucin glycoprotein as a homogeneous cylinder, for which a Guiner analysis suggested that the length of the glycosylated regions was ~100 nm with a radius of 24 ± 1 nm. Subsequently, they reanalyzed their SANS data in light of the SAXS study[10] and invoked a dumbbell model in which two globular structures (with dimension 10−20 nm) are connected by a 40−50 nm glycosylated spacer with a thickness of a few nanometers.

A more complex form factor approach has been adopted here that embodies the essence of the dumbbell model, in which the scattering has been analyzed using a model that comprises two main scattering terms

$$I(Q) = I(Q)_{\text{peptidebackbone}} + I(Q)_{\text{globule}} \quad (3)$$

The first term of eq 3 is the contribution from the glycosylated peptide backbone (Scheme 1), whereas the second term accounts

Scheme 1. Solution Conformation of Mucin Comprising Hydrophobic Globules Connected by a Glycosylated Spacer[a]

[a] Hydrophobic globules are modeled in terms of a dispersion of polydisperse spheres, whereas the spacer gives rise to a Q^{-2} contribution to the overall scattering (adapted from ref 10).

for the dispersion of hydrophobic globules connected by the glycosylated peptide backbone. The peptide backbone is modeled as

$$I(Q)_{\text{peptidebackbone}} = \frac{I_1}{\xi^2 Q^2} + \frac{I_2}{\zeta^4 Q^4} \tag{4}$$

where the intensities I_1 and I_2 characterize the contribution to the scattering arising from the peptide backbone with characteristic length scale ξ (where $\xi^2 Q^2 > 1$) and from some larger, ill-defined structure, ζ.

The second term in eq 3, $I(Q)_{\text{globule}}$, is responsible for the scattering from the locally ordered hydrophobic globules, and it was deemed most appropriate to model this structure as a concentrated dispersion of uncharged (polydisperse) spheres given (i) the liquid ordering scaling of the peak positions with concentration and (ii) the fact that no change in scattering is observed as a result of the increase in the ionic strength (Figure S5 in the Supporting Information). Therefore,

$$I(Q)_{\text{globule}} = NV^2(\rho_m - \rho_s)^2 P(Q)S(Q) \tag{5}$$

where N is the number of scatterers of volume, V, per unit volume and $(\rho_m - \rho_s)^2$ is their contrast against the solvent. The form factor $P(Q)$ is calculated using a distribution of polydisperse spherical scatterers with

$$P(Q) = 3\left[\frac{\sin QR - QR\cos QR}{(QR)^3}\right]^2 \tag{6}$$

integrated over a modified Schulz distribution

$$n(R) = \left[\frac{(Z+1)}{(\bar{R} - R_1)}\right]^{Z+1}(R - R_1)^Z \frac{\exp\left[\frac{-(Z+1)}{(\bar{R} - R_1)(R - R_1)}\right]}{\Gamma(Z+1)} \tag{7}$$

with width $\sigma = ((\bar{R} - R_1))/((Z+1)^{1/2})$ to account for variation in size.

This model, idealized in Scheme 1 with the various contributions to the overall fit illustrated in Figure 1, is most sensitive to the position of the peaks, allowing the size, R, and volume fraction, ϕ (= NV), of the globules to be readily parametrized ($R \approx 10-15$ nm, $\phi \approx 0.30$ to 0.40), yielding values that are in very good agreement with those obtained by Waigh et al.[10] The Q^{-2} contribution to the overall fit can be reanalyzed representing the data in a Zimm plot to yield a correlation length of ~13 (±1) nm (and over the high Q limit, $R_g \approx 9$ (±1) nm). This observation is consistent with previous reports of a swollen coil, commensurate with the type of structure envisaged by Waigh as a glycosylated spacer. As may be seen, the Q^{-4} term contributes rather weakly to the overall fit; indeed, the fit is dominated by the Q^{-2} and globule terms. Therefore, there is also a resonance of this model with the "bottle brush" and "zipper" models,[17] which lends support to and gains credence from the aforementioned various models used previously to describe the solution conformation of mucin.

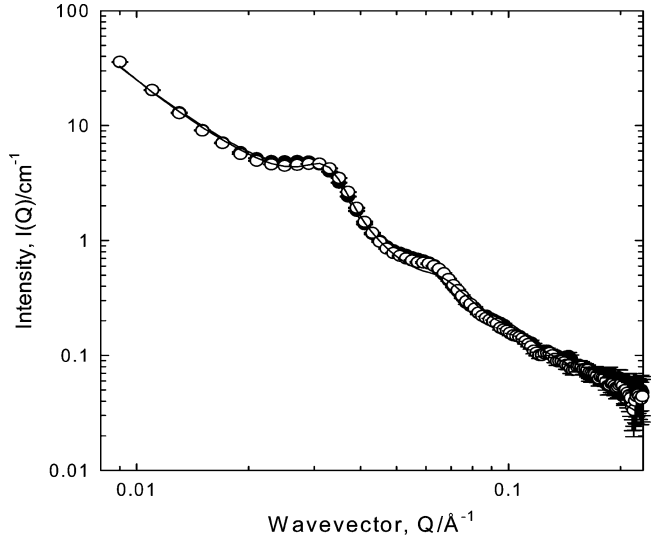

Figure 2. Scattering from 5 wt % mucin in the absence (closed circles) and in the presence of 0.5 wt % deuterated PEG10K g mol^{-1} (open circles) at 37 °C, pH 7. The lines correspond to the fits to the model described in the text.

Upon dilution from [mucin] = 5 to 1 wt %, the peak in the data moves to lower Q ($\xi \propto c^{-0.38\,(\pm 0.03)}$). The peak position corresponds to a distance of 21 nm at 5 wt % mucin increasing to 39 nm at 1 wt % mucin. The scattering from 5 wt % mucin solutions over a pH range of 2 < pH< 9 (at 37 °C) (Figure S6 in the Supporting Information) showed identical maxima, indicating that the conformation of the mucin does not change over this pH range, in contradiction to that observed by Cao et al.[18] However, the sample at pH 2 did exhibit slightly different scattering: the intensity of the maxima is slightly reduced, but there is no change in the peak position. This observation confirms what is known about commercial PGM samples: the extraction process disrupts the disulfide bridges, leading to a much weaker sol−gel transition around pH < 4 and the lack of gel formation. The Supporting Information also presents supporting viscosity studies (Figure S2 in the Supporting Information).

SANS from PGM Solutions in the Presence of the Polymers. The scattering from 5 wt % PGM solutions (37 °C) in the presence of 0.5 wt % *l*-PEG10K, *b*-PEG20K, and *l*-PEG100K showed no significant differences from the 5 wt % PGM solution. A typical data set is presented in Figure 2. A deuterated *l*-PEG10K was used, so no scattering is observed from this polymer in D_2O, the so-called "contrast match" condition. For the other polymers, the concentration was too low to detect measurable scattering. The simplest interpretation of this observation is the lack of an interaction between the mucin and the various PEGs, at least to a degree that induces a structural perturbation in the mucin. The same observations were made for all pHs examined, viz., pH 2, 7, and 9 (Figure S7 in the Supporting Information presents as exemplar the pH 2 data). Similarly, there is no change in the (relative) viscosity of the mucin solutions upon the addition of the PEG (Figure S8 in the Supporting Information).

The addition of 0.5 wt % PAMAM dendrimers (amino-terminated G2.0 and G4.0, carboxylic acid terminated G3.5 and G5.5) to 5 wt % mucin solutions did induce changes in the mucin scattering, as exemplified in Figure 3, indicating an

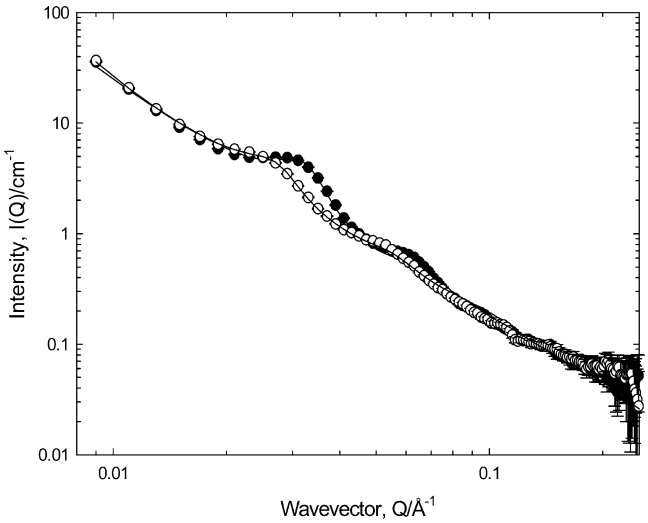

Figure 3. Scattering from 5 wt % mucin in the absence (closed circles) and in the presence of 0.5 wt % PAMAM dendrimer G2.0 (open circles) at 37 °C, pH 7. The lines correspond to the fits to the model described in the text.

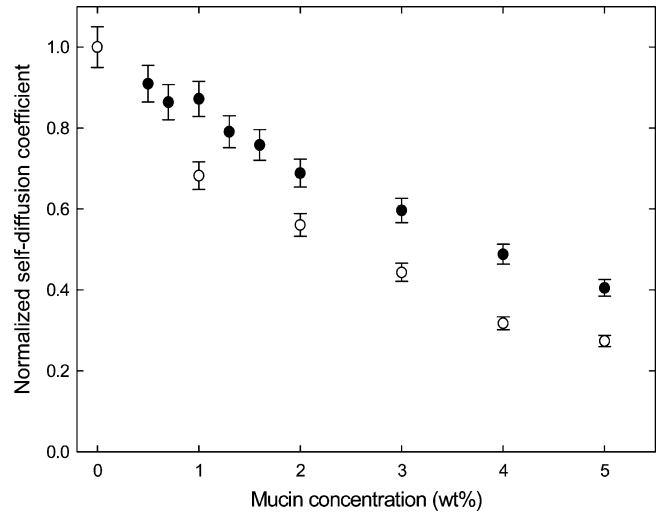

Figure 4. Normalized self-diffusion coefficients of 0.5 wt % PEG10K g mol^{-1} (closed circles) and PEG100K g mol^{-1} (open circles) in mucin solutions at 37 °C, pH 7.

interaction between these polymers and mucin. These changes were pH-dependent. Any contribution to the scattering from the PAMAM has been ignored because there was no measurable scattering in the absence of the mucin. The scattering from 0.5 wt % G2.0 (and G4.0) in 5 wt % mucin did not show any major change from the 5 wt % mucin scattering for pHs 2 and 9 (Figure S9 in the Supporting Information presents the pH 9 data), whereas a perturbation was observed at pH 7, Figure 3. Similar trends were observed in the viscosity behavior (Figures S10 and S11 in the Supporting Information).

The most obvious change is the shift of the maxima to lower Q. This indicates that the separation of the structures giving rise to these features has increased. Analogous behavior was observed for PAMAM G4.0.

In the case of the half-generation dendrimers, G3.5 (Figure S12a,b,c in the Supporting Information) and G5.5 (data not presented), a similar modulation of the scattering was observed but with three notable differences: (i) the change in scattering exhibited a rather different pH profile, viz., there was no change induced by the dendrimer at pH 2, but perturbations were evident at pH 7, which become more pronounced at pH 9; (ii) the peaks moved in the opposite direction, that is, toward higher Q values, indicating a decreasing separation of scatterers; and (iii) there appears to be slight drop in scattering intensity in the presence of the dendrimer, which increases with the strength of the interaction (no such change was observed in the G2.0 and G4.0 cases). Analogous behavior was observed for PAMAM G5.5. "Signature" pH effects were also observed when *b*-PEI2K (Figure S13 in the Supporting Information) was added to the 5 wt % mucin solutions (the changes in the perturbations in the scattering were much more pronounced that the PAMAM G2.0 and G4.0 dendrimer cases): no change in scattering at pH 2 but a much larger difference in scattering at pH 7. The presence of *b*-PEI25K caused flocculation of the mucin solutions; therefore, this system was not further studied but serves to underline the importance of the relative signs and magnitudes of the respective charge in these systems.

PGSE-NMR Study on Mucin Solutions in the Presence of Probe Polymers. The diffusion of a series of probe polymers (at fixed polymer concentration, 0.5 wt %) in a range of mucin solutions (0 < [mucin] < 5 wt %) has been examined at 37 °C. All polymers showed a decrease in the diffusion rate with increasing mucin concentration. Therefore, it is important to separate the effects of any specific interactions (e.g., binding) from that arising as a result of simple obstruction, namely, that the probe polymers have to diffuse around the mucin and there is the concomitant increase in diffusion path length. Additionally, there is the complication that the probe polymers are inherently of different molecular weights, and this will also affect their absolute diffusion rates.

Figure 4 presents representative normalized self-diffusion coefficients of *l*-PEG10K and *l*-PEG100K in mucin solutions, these being normalized to the measured self-diffusion coefficient of the PEG in free solution, that is, when [mucin] = 0 wt %. The diffusion of both *l*-PEG10K and *l*-PEG100K decreases with increasing mucin concentration because for [mucin] = 0, $D_s^{(10K)} > D_s^{(100K)}$ by a factor of 3.5 (Figure S14 in the Supporting Information), which is consistent with the 10× decrease in molecular weight. The normalized diffusion data should at least to a first approximation remove the inherent effect of molecular weight and permit a comparison of the retardation induced by the mucin.

The (normalized) diffusion of 0.5 wt % PAMAM G2.0 and G4.0 shows a complex dependence on [mucin] and pH (Figure 5) in a fashion reminiscent of the characteristic profile observed in the SANS experiment. In particular, the data revealed a higher diffusion rate in mucin solutions at pH 9 (Figure 5) when compared with the diffusion of these probe polymers in mucin at pH 7 (Figure 5), suggesting that the same complex pH-dependent interaction between the dendrimers and the mucin is observable in the diffusion data. Analogous behavior was observed for G3.5 and G5.5. Furthermore, the diffusion of *b*-PEI2K was strongly retarded in mucin, interpreted as a very strong interaction between the dendrimer and the mucin. A manifestation of this strength of interaction was the short "shelf-life" of *b*-PEI25K/mucin samples, which phase separated after just a few hours.

A wider family of polymers has been examined by PGSE-NMR than has been possible by SANS, including dextrin, but over a more focused pH range. The conclusions of this larger study are presented in the bar-chart representation of Figure 6, where the normalized self-diffusion coefficients have been tabulated at one representative mucin concentration, 3 wt %.

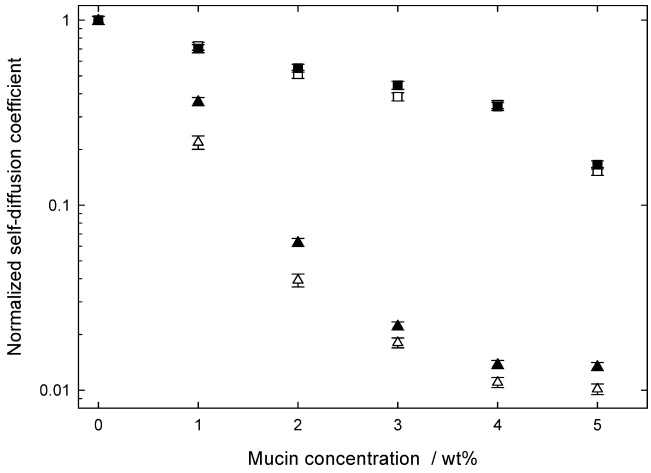

Figure 5. Normalized self-diffusion coefficients of 0.5 wt % PAMAM dendrimer G2.0 (open symbols) and G4.0 (filled symbols) at pH 9 (squares) and pH 7 (circles) in mucin solutions and 37 °C.

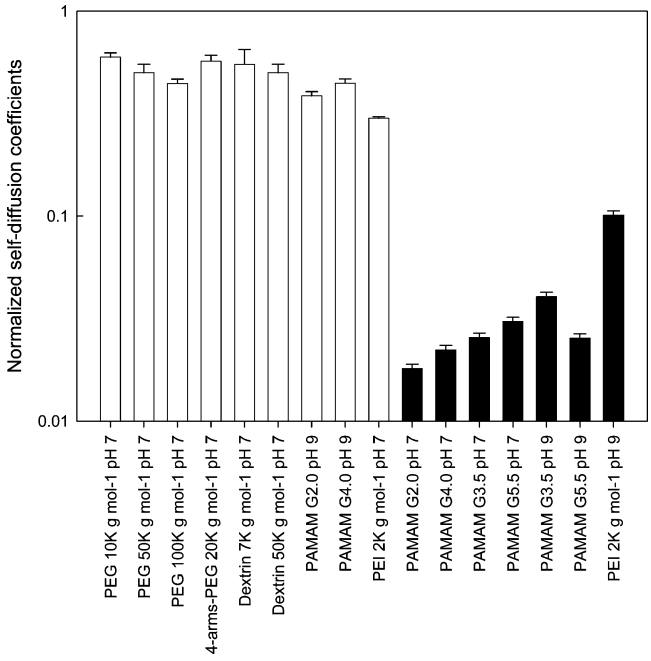

Figure 6. Bar chart of the normalized self-diffusion coefficients of all probe polymers in aqueous 3 wt % mucin solutions. The unshaded bars correspond to those systems for which SANS confirmed the lack of an interaction whereas the shaded bars correspond to interacting systems.

Discussion

For all polymer−mucin samples explored, the SANS and PGSE-NMR experiments gave complementary insight into the interaction of the probe polymer with the mucin. The nonionic polymers (dextrin 7K, dextrin 50K, *l*-PEG10K, *l*-PEG50K, *l*-PEG100K, 4-arms-PEG20K) displayed a behavior consistent with there being no interaction with the mucin; there was no change in the scattering profile, and one may therefore conclude that the moderate retardation in the diffusion arises simply because of the obstruction effect. There is the obvious molecular weight dependence to consider when discussing the absolute diffusion rates, but the normalized diffusion rates suggest no specific molecular-weight-dependent interaction with mucin. A similar study by Lafitte et al.[19,20] on the effect of PGM on the diffusion of PEG as a function of pH, ionic strength, and temperature demonstrated that pH imparted a stronger impact on the PEG diffusion rate compared with that due to ionic strength and temperature, reflecting the underlying changes in mucin network homogeneity and viscosity. Furthermore, Lai et al.[21] found from their particle-tracking measurements that the diffusion of nanoparticles through mucin showed a complex dependence on particle size, but those particles coated with low-molecular-weight PEG diffused through mucus only slightly slower (×4−6) than in pure water. The same group[22] later showed that higher molecular weight PEGs led to mucoadhesion, highlighting the complexity of studying these systems, but would be consistent with the observation here of the slightly reduced normalized diffusion coefficient for the PEG 100K g mol^{-1} sample compared with the PEG 10K g mol^{-1} one.

The PAMAM dendrimers experienced a significant retardation in their diffusion within the mucin solutions (sometimes close to an order of magnitude) but under conditions where the PAMAM and mucin bore opposite charge. Concomitantly, there was a movement of the peak in the SANS data. Changing the pH to reverse the charge on either mucin or probe polymer "turned off" the interaction. The mechanism of interaction appears, therefore, to be driven by electrostatic interactions.

For the amino-terminated PAMAMs (G2.0 and G4.0) at pH 7, the amine groups are largely protonated (positively charged), whereas the mucin glycoprotein is deprotonated and negatively charged (via the carboxylic acid groups of the protein backbone ($pK_a \approx 3.9$ to 4.1) and the side groups of sialic acid ($pK_a \approx 2.6$), sulfated glucosamine, and galactoamines ($pK_a \approx 1$)), leading to the observed strong electrostatic interaction. The peak in the scattering moves to lower Q values, indicating that the separation of the scattering centers has increased. It is hypothesized that the PAMAM binds electrostatically to the oppositely charged mucin monosaccharide side chains, driving an expansion of the glyscoylated spacer, thus pushing the globules further apart. At pH 2, the amine groups are completely protonated (+ve charged), but the mucin is also partially positively charged (IEP = 2 to 3), and accordingly, no interaction is observed.

In contrast, for the half-generation PAMAMs (G3.5 and G5.5) at pH 7, the terminating carboxylic acid groups are already moderately deprotonated (i.e., negatively charged), and whereas the mucin is also negatively charged, surprisingly an interaction is still observed. This interaction becomes more pronounced at pH 9, that is, where the negative charge on the mucin is further increased. (No interaction is seen at pH 2.) Now, the peak in the SANS pattern has moved to higher Q, indicating that the separation of the globules has decreased. Clearly, a different mechanism is operating in the full- and half-generation PAMAMs. The origin of this interaction is most likely to be hydrogen bonds between the charged carboxylic acid groups on the PAMAM and the sugar residues on the monosaccharide side chains, leading to a collapse of the glysocylated spacer as the PAMAM induces bridging between adjacent saccharide structures.

Conclusions

The structure of aqueous probe polymer−mucin solutions has been explored by SANS, viscosity, and pulsed-gradient spin−echo NMR (PGSE-NMR). The SANS data provide a simple measure of the occurrence and nature of any interaction between the probe polymer and the mucin. The diffusion and viscosity data provide complementary insight into these systems. The scattering data were found to be most appropriately analyzed by a model describing the mucin as a dispersion of polydisperse spherical scatterers with a typical size of ∼10 nm distributed throughout a polymeric matrix. Nonionic polymers such as

l-PEG10K and *l*-PEG100K did not interact with the mucin and caused no change in the bulk viscosity of the mucin/PEG solution but suffered a moderate retardation in their diffusion through the mucin. A pH-dependent interaction was found for a series of PAMAM dendrimers and PEI, exposing a strong electrostatic interaction. This study has shown that it is possible to distinguish and separate the effects of specific interactions between the probe polymer and mucin from simple obstruction effects. These conclusions should direct the choice of polymer structure to be adopted when designing polymer-based delivery systems for the delivery through such mucin-rich environments.

Acknowledgment. This study was supported by Cardiff University in the form of a Richard Whipp studentship. STFC is thanked for providing neutron beam time at ISIS. EPSRC is also acknowledged for the provision of a Platform grant (EP/C013220/1).

Supporting Information Available. Additional small-angle neutron scattering, viscosity, and NMR data (as referred to in the text). This material is available free of charge via the Internet at http://pubs.acs.org.

References and Notes

(1) Vicent, M. J.; Ringsdorf, H.; Duncan, R. *Adv. Drug Delivery Rev.* **2009**, *61*, 1117–1120.
(2) Sanders, N.; Rudolph, C.; Braeckmans, K.; De Smedt, S. C.; Demeester, J. *Adv. Drug Delivery Rev.* **2009**, *61*, 115–127.
(3) Bansil, R.; Turner, B. S. *Curr. Opin. Colloid Interface Sci.* **2006**, *11*, 164–170.
(4) Raynal, B. D. E.; Hardingham, T. E.; Sheehan, J. K.; Thornton, D. J. *J. Biol. Chem.* **2003**, *278*, 28703–28710.
(5) Hong, Z. N.; Chasan, B.; Bansil, R.; Turner, B. S.; Bhaskar, K. R.; Afdhal, N. H. *Biomacromolecules* **2005**, *6*, 3458–3466.
(6) Adikwu, M. U. *Bio. Pharm. Bull.* **2005**, *28*, 1801–1804.
(7) Hannig, M.; Herzog, S.; Willigeroth, S. F.; Zimehl, R. *Colloid Polym. Sci.* **2001**, *279*, 479–483.
(8) Glantz, P. O. J.; Arnebrant, T.; Nylander, T.; Baier, R. E. *Acta Odontol. Scand.* **1999**, *57*, 238–241.
(9) Jay, G. D.; Haberstroh, K.; Cha, C. J. *J. Biomed. Mater. Res.* **1998**, *40*, 414–418.
(10) Di Cola, E.; Yakubov, G. E.; Waigh, T. A. *Biomacromolecules* **2008**, *9*, 3216–3222.
(11) Griffiths, P. C.; Cheung, A. Y. F.; Davies, J. A.; Paul, A.; Tipples, C. N.; Winnington, A. L. *Magn. Reson. Chem.* **2002**, *40*, S40–S50.
(12) Stilbs, P.; Paulsen, K.; Griffiths, P. C. *J. Phys. Chem.* **1996**, *100*, 8180–8189.
(13) Papagiannopoulos, A.; Fernyhough, C. M.; Waigh, T. A.; Radulescu, A. *Macro. Chem. Phys.* **2008**, *209*, 2475–2486.
(14) Yakubov, G. E.; Papagiannopoulos, A.; Rat, E.; Easton, R. L.; Waigh, T. A. *Biomacromolecules* **2007**, *8*, 3467–3477.
(15) Yakubov, G. E.; Papagiannopoulos, A.; Rat, E.; Waigh, T. A. *Biomacromolecules* **2007**, *8*, 3791–3799.
(16) Waigh, T. A.; Papagiannopoulos, A.; Voice, A.; Bansil, R.; Unwin, A. P.; Dewhurst, C. D.; Turner, B.; Afdhal, N. *Langmuir* **2002**, *18*, 7188–7195.
(17) Carlstedt, I.; Sheehan, J. K. *Biorheology* **1984**, *21*, 225–233.
(18) Cao, X. X.; Bansil, R.; Bhaskar, K. R.; Turner, B. S.; Lamont, J. T.; Niu, N.; Afdhal, N. H. *Biophys. J.* **1999**, *76*, 1250–1258.
(19) Lafitte, G.; Soderman, O.; Thuresson, K.; Davies, J. *Biopolymers* **2007**, *86*, 165–175.
(20) Lafitte, G.; Thuresson, K.; Soderman, O. *J. Pharm. Sci.* **2007**, *96*, 258–263.
(21) Lai, S. K.; O'Hanlon, D. E.; Harrold, S.; Man, S. T.; Wang, Y. Y.; Cone, R.; Hanes, J. *Proc. Natl. Acad. Sci. U.S.A.* **2007**, *104*, 1482–1487.
(22) Wang, Y. Y.; Lai, S. K.; Suk, J. S.; Pace, A.; Cone, R.; Hanes, J. *Angew. Chem., Int. Ed.* **2008**, *47*, 9726–9729.

BM9009667